UCRL-JRNL-219323

LAWRENCE
LIVERMORE
NATIONAL
LABORATORY

Thomson-scattering measurements of high electron temperature hohlraum plasmas for laser-plasma interaction studies

D. H. Froula, J. S. Ross, L. Divol, N. Meezan, A. J. MacKinnon, R. Wallace, S. H. Glenzer

February 27, 2006

Physics of Plasmas

Thomson-scattering measurements of high electron temperature hohlraum plasmas for laser-plasma interaction studies

D. H. Froula,* J. S. Ross,† L. Divol, N. Meezan,
A. J. MacKinnon, R. Wallace, and S. H. Glenzer
L-399, Lawrence Livermore National Laboratory,
P.O. Box 808, Livermore, CA 94551, USA

(Dated: February 6, 2006)

Abstract

Accurate measurements of the plasma conditions in laser-produced high-temperature plasmas have been achieved using the recently activated 4ω Thomson-scattering diagnostic at the Omega Laser Facility. These diagnostic measurements were performed in a new hohlraum target platform that will be used to study laser-plasma interaction in a strongly damped regime comparable to those occurring in indirect drive inertial confinement fusion plasmas. The Thomson-scattering spectra show the collective ion-acoustic features that fit the theory for two ion species plasmas allowing us to accurately and independently determine both the electron and ion temperatures. The electron temperature was found to range from 2 keV to 4 keV as the total heater beam energy deposited into the hohlraum was increased from 8 kJ to 17 kJ. The results are compared to 2D hydrodynamic simulations using flux limited diffusion and nonlocal heat flux models. The target platform presented provides a novel test bed to investigate laser-plasma interaction physics in the strongly damped backscatter regime.

PACS numbers: 52.25.Os, 52.35.Fp, 52.50.Jm

*Electronic address: `froula1@llnl.gov`
†Also at Department of Applied Science, University of California at Davis.

I. INTRODUCTION

Inertial confinement fusion and high energy density science experiments require direct and accurate measurements of the plasma conditions. In the indirect drive approach to inertial confinement fusion (ICF), high-Z hohlraums are used as radiation enclosures converting high-power laser energy into a soft x-ray radiation field that drives the fusion capsule implosion by x-ray ablation pressure [1]. For achieving a symmetric capsule implosion and for reaching ignition conditions, it is required that the energetic laser beams efficiently propagate and create soft x rays close to where they were initially pointed on the hohlraum wall. The inside of the hohlraum will be filled with low-Z or mid-Z plasmas from the initial fill material, ablated material off the capsule, and other lined hohlraum surfaces. The fill plasma reduces the inward motion of the high-Z plasma wall thus obtaining a highly symmetric soft x-ray radiation pressure for symmetric high-convergence implosions. The physics of laser beam propagation in these ignition hohlraums is largely dominated by the laser-plasma interactions in the fill plasma where laser backscattering, beam deflection, beam filamenation, and self focusing may occur when driving these parametric instabilities beyond their thresholds [**?**].

To determine these thresholds and to model the laser-plasma interaction processes a new hohlraum platform has been developed. Thomson scattering is used to accurately determine the plasma parameters in this target platform and is compared with hydrodynamic simulations. In high-electron-temperature hohlraum plasmas, present capacities to predict the plasma conditions are limited by the approximations in heat transport modeling. Although recent code developments make use of nonlocal modeling and magnetic field packages, only few tests of these codes exist and direct measurements of the plasma conditions with Thomson scattering are required to be confident in predicting target performance [2].

In this paper we report on the characterization of a recently designed laser-plasma interaction target platform that provides a uniform 2 mm long high-temperature ($T_e = 3.5 - 4.0$ keV) plasma interaction region that is comparable to the interaction region in an ignition hohlraum. This platform is a significant improvement over gasbag [2**?**] or toroidal hohlraum [3] targets that have previously been used to study laser-plasma interactions.

Electron temperatures in open geometry gas bag plasmas with roughly the same length and density shot at the old NOVA facility reached 2.8 keV using significantly more energy on target than is currently available [2]. Experiments at the Omega Laser Facility using

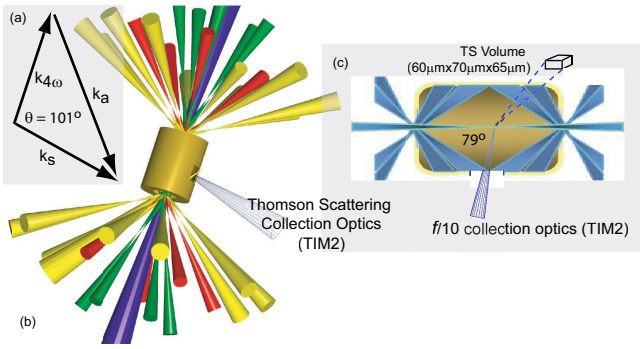

FIG. 1: (a) The ion-acoustic wave vector probed by Thomson scattering is defined by the scattering geometry. (b) The 37 heater beams are distributed into three cones; 18 58° cone 3 beams (yellow), 9 42° cone 2 beams (red), 10 21° cone 1 beams (green). The 4ω probe beam is aligned along the hohlraum axis. A 500 micron square window cut into the side of the hohlraum wall allows light scattered from a small scattering volume located at the center of the hohlraum to be collected by an optical Thomson-scattering system. (c) The heater beams are focused on the high-Z hohlraum wall creating soft x-rays that heat the hohlraum fill material (CH gas or SiO_2 foam).

gasbag plasmas have resulted in a considerably lower plasma temperature of ~ 1.8 keV [4]. The gas bag targets produce a much lower electron temperature than the new hohlraum platform due to the larger volume of plasma heated when using spherical target geometry and the lower available heater beam energy when shooting into a gas bag at the Omega Laser Facility. The laser-plasma interaction physics in the low temperature regime is significantly different from that expected at ignition conditions. At high temperatures, the propagation to the hohlraum wall is predicted to be improved; increasing electron temperature will reduce filamentation, beam spray, and stimulated backscattering process, therefore, increasing the total transmission to the hohlraum wall. The target platform presented in the present study will provide a novel test bed to investigate laser-plasma interaction physics at electron temperatures (3 keV to 4 keV) and scale-lengths (2 mm) approaching ignition conditions.

The plasma conditions are measured at the center of hohlraums filled with either CH-gas or SiO_2 foam using Thomson scattering and are compared to hydrodynamic simulations that employ either a nonlocal or flux limited model. The electron temperature is scaled from 2 keV to 4 keV by varying the energy deposited into the hohlraum from 8 kJ to 17 kJ; this scaling is consistent with assuming the power is deposited at the critical surface and balancing the incident laser flux with the heat conduction into the hohlraum wall [5].

Section II presents the experimental setup where the laser beam configuration, diagnostic setup, and simulation details are presented. Comparison between the experimental results the hydrodynamic simulations are presented in Sec. III. The paper is concluded in Sec. IV.

II. EXPERIMENTAL SETUP

A. Target and Beam Configuration

The experiments were performed with the Omega Laser Facility at the Laboratory for Laser Energetics. The laser facility consists of 60 frequency tripled Nd:glass laser beams with approximately 500 J per beam of 351 nm (3ω) laser light on target [6]. One of the 3ω beams (B25) has been de-tuned to produce 2ω light and directed to a new port (P9) and subsequently doubled to provide a 4ω Thomson-scattering probe laser [7]. The targets are heated with 37 3ω beams with total energies of 8 kJ to 17 kJ in a 1 ns flat top laser pulse with 0.1 ns rising and falling edges. These targets are gas-filled (1 atm of 1% Ar, 29% CH_4, 70% C_3H_8) or foam-filled (1 mg/cc SiO_2) hohlraums with a length of 2 mm and a diameter of 1.6 mm (Fig. 1). The heater beams penetrate the hohlraum at both ends through laser entrance holes with a diameter of 0.8 mm which are covered with 0.35 micron thick polyimide membranes when a gas fill is employed. The hohlraums are aligned along the propagation direction of the 4ω probe beam (P9 axis).

B. Hydrodynamic Modeling

The results of these experiments demonstrate electron temperatures approaching 4 keV and are also used to benchmark and gain confidence in the hydrodynamic modeling used to design ICF targets for the NIF. Few quality measurements of the electron temperature in high temperature laser plasmas exist to test heat transport physics [8]. In this paper, experimental results are compared with hydrodynamic modeling performed in two dimensions using the code HYDRA [9] where the heat flux is determined by either a flux limited diffusion model or a nonlocal model. Figure 2 shows that both models indicate a peak electron temperatures in the range of 3 keV to 4 keV along a 2 mm long flat density plateau following the hohlraum axis, but there are significant differences in the temperature profiles between the models.

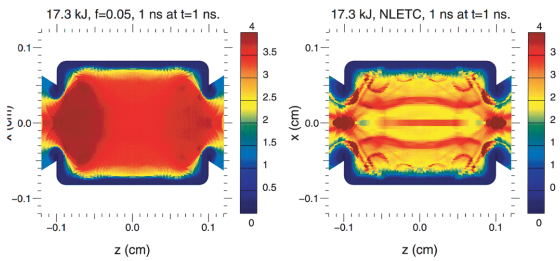

FIG. 2: (a) Simulations using a flux limited diffusion model (f=0.05) show a uniform 3.5 keV temperature profile along the hohlraum axis at the end of the heater beams (t=1.0 ns). (b) Calculations employing a nonlocal heat transport model show large temperature gradients around the laser beams. The left hand side of the hohlraum shows slightly higher temperatures because there are 3 additional heater beams on that side. A total heater beam energy of 17 kJ and a 1-atm-CH gas fill is used in these simulations.

Figure 2(a) shows calculations using a classical heat transport model where a flux limiter (f=0.05) is used to limit the heat flux. The CH gas is homogeneous heated to a peak temperature of 3.5 keV. The flux limited diffusion model uses classical linear Spitzer-Harm heat transport [10] where the heat flux is estimated by the gradient in the electron temperature multiplied by the conductivity (κ) [11],

$$\mathrm{q}_{SH} = \kappa \nabla \mathrm{T}_e \tag{1}$$

This equation is developed assuming small deviations from a Maxwellian distribution confining the validity of the model to when the electron mean free path is much smaller than the temperature gradient scale length ($\lambda_T = T_e/\nabla T_e$). Studies have shown that in order for classical Spitzer-Harm simulations to be consistent with experiments the heat flux must be limited [**?**]. Furthermore, Eqn. 1 can predict an unphysical heat flow; the heat can propagate faster than the physical upper limit given by free streaming value ($\mathrm{q}_{fs} = \mathrm{n}_e \mathrm{T}_e \mathrm{v}_e$), therefore, the flux limited diffusion model in HYDRA calculates the heat flux following,

$$\mathrm{q} = \min[\mathrm{q}_{SH}, \mathrm{f}\ \mathrm{q}_{fs}], \tag{2}$$

where the heat flux (q) is calculated using the minimum between the classical Spitzer-Harm flux and a fraction (f) of the free streaming flux. Various processes can explain the need for a flux-limiter: self-generated magnetic fields [12**?**], plasma turbulance [**?**], nonlocal nature

of the heat flux [13] and other processes that limit the electron-ion collision rate. The flux limiter is a single value and is not valid for all conditions within the simulation but has been shown to provide a reasonable approximation in large simulations were detailed physics is unknown or too computationally expensive [**?**].

Figure 2(b) shows calculations that use a nonlocal transport model described in Ref. [14]. These simulations show steeper gradients than the heat flux model particularly around the laser entrance hole where several beams overlap. Such gradients have also been experimentally observed in previous Thomson-scattering measurements on the Nova laser facility [15].

Advancements in computations has recently allowed nonlocal models to be implemented where the calculated heat flux takes into account the heat flux resulting from the long mean free path of the high velocity electrons. The nonlocal model uses the electron temperature profile over a volume enclosed by a few hundred mean free paths to calculate the heat flux eliminating the need for an unphysical flux limiter. Although the nonlocal model is still not derived from first principles it is based on sound physical concepts and it seems to captures the essential physics when compared with kinetic simulations. The general behavior of the nonlocal model, like the one in HYDRA, is to reduce the heat flux as compared with the flux calculated by a flux limited diffusion model as the temperature-scale-length gets smaller compared to the electron mean free path.

The primary difference between the nonlocal and flux limited models is the ability for the nonlocal model to inhibit the heat flux where there are large gradients while still allowing the fast electrons to carry away the heat. For example, in the presence of large temperature gradients, the flux limited model tends to either over estimate the heat flux (large flux limiter) artificially reducing the temperature gradient, or under estimate the heat flux (small flux limiter) therefore, preventing the surrounding plasma from getting hot. In our simulations both models provide reasonably close electron temperatures at the center of the hohlraum, but the nonlocal model shows larger temperature gradients resulting from the local laser beam heating that tends to reduce the calculated heat flux, therefore, increasing the temperature inside of the laser beams. Although the flux limited model agrees with the nonlocal model in some regions, a more comprehensive model may be necessary to sufficiently design indirect drive targets due to the sensitivity of laser plasma interaction thresholds to detailed plasma parameters.

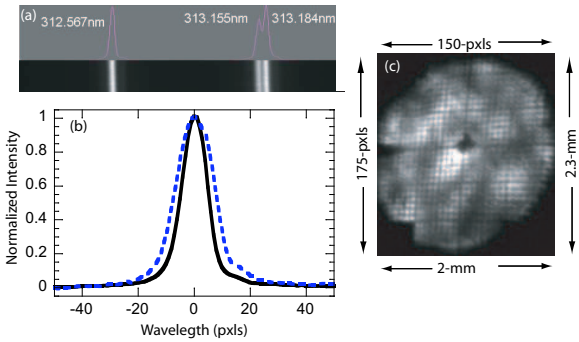

FIG. 3: (a) Hg spectral lines where used to measure the spectral dispersion. (b) Using the Hg spectral lines, the instrument resolution was measured for a 100 μm (line) and 200 μm (dashed) slit width. (c) An image of a grid with line spacing of 63.5 μm is located at TCC. The lines are aligned parallel to the axis of the probe beam and imaged through the Thomson-scattering system.

C. Thomson scattering Diagnostic

Thomson-scattering measurements use an optical laser with a frequency (ω_o) and a wave number (k_o) to scatter from electron density fluctuations with a given wave vector (k_a). Collective Thomson scattering is used as a diagnostic to probe ion-acoustic fluctuations when the probed electrons follow the motion of the ions ($\mathrm{ZT}_e/\mathrm{T}_i > k_a^2\lambda_{De}^2$).

The scattered frequency spectrum provides a measure of the local particle flow velocity and the ion-acoustic sound speed that is directly related to the electron temperature. In our multi-ion-species carbon-hydrogen plasmas, the relative amplitude of the light scattered from ion-acoustic waves allows an accurate determination of the ion temperature [16–19]. In theory, the ion temperature can also be obtained from the width of the intensity peaks in the Thomson-scattering spectra, but velocity and temperature gradients within the scattering volume make this measurement uncertain and therefore, unreliable in laser-produced plasmas. Our experiments in high temperature CH gas plasmas are able to accurately measure the electron temperature using the frequency of the ion-acoustic modes, and the ion temperature using the relative damping of the carbon-like and hydrogen-like modes.

Typical 4ω probe beam energies of E=200 J with a flat 1 ns pulse duration have been employed with a small focal spot of 60 μm at the Thomson-scattering volume (Figure 1(b)). The scattered light is imaged, at a scattering angle of $\theta = 101^o$, through a diagnostic window (500 μm$\times$500 μm) cut in the side of the hohlraum wall. The hole is covered with a 0.26

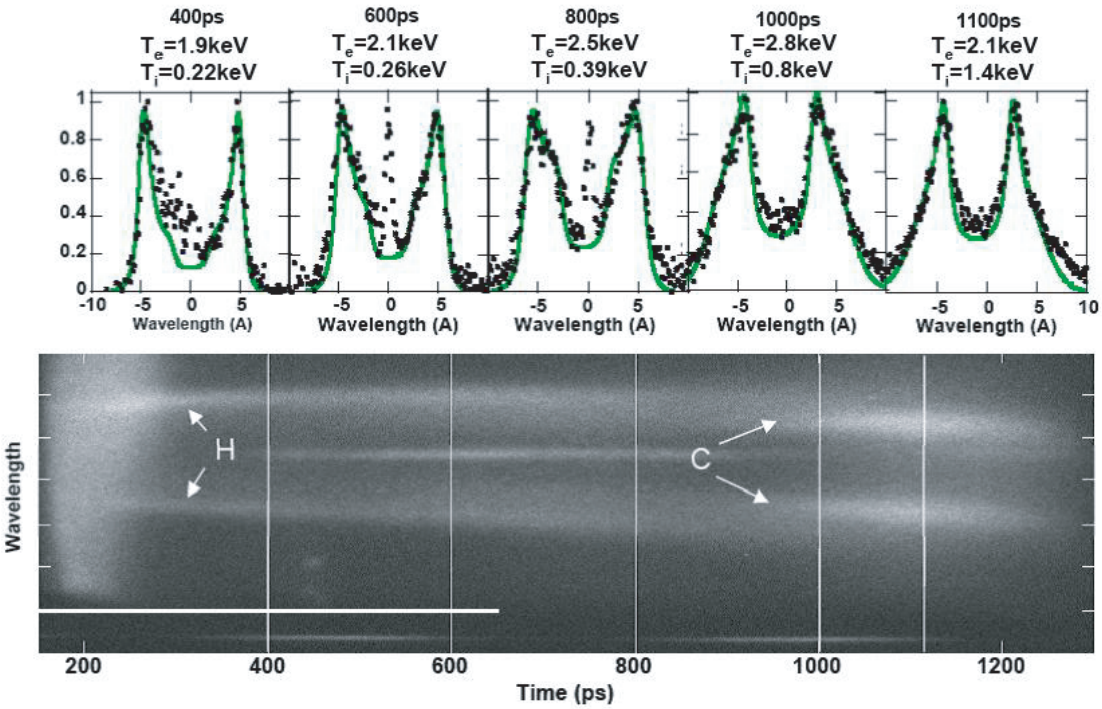

FIG. 4: (a) The streaked Thomson-scattering spectrum shows a heavily damped carbon-like mode and a weakly damped hydrogen-like mode early in time. The damping of the modes is reversed by the end of the probe beam. The spectra are fit to determine T_e, T_i, and n_e at selected times (b) 400 ps, (c) 600 ps, (d) 800 ps, (e) 1000 ps, (f) 1100 ps.

micron thick polyimide window when a gas fill is employed. The scattering parameter is $\alpha = 1.4$ for plasma conditions of $T_e = 4$ keV and $n_e = 6 \times 10^{20}$ cm^{-3} where the scattering parameter is defined,

$$\alpha \equiv \frac{1}{k_a \lambda_{De}} = 1 \times 10^{-10} \left(\frac{n_e[\mathrm{cm}^{-3}]}{T_e[\mathrm{keV}]} \right)^{1/2} \tag{3}$$

In our experiment T_i/ZT_e is always greater than the square of the scattering parameter ($\alpha^2 > T_i/ZT_e$), therefore, collective ion-acoustic modes are observed.

The collection system was designed to be achromatic between 250 nm and 600 nm to allow for Thomson-scattering studies over a range of scattered wavelengths. Scattered light is collected and collimated by an $f/10$ achromatic lens with a 50 cm focal length. A blast shield with a coating to reject the scattered light from the 3ω heater beams has been implemented prior to the collection lens. A 10 cm focusing mirror with a 50 cm focal length images the scattered light onto the 150 μm slit of a 1-meter imaging spectrometer with a 3600 lines/mm grating. A high dynamic range streak camera is coupled to the spectrometer through a

200 μm temporal slit.

The spectral resolution was measured using Hg lines around 310 nm to have a FWHM=0.05 nm using a 100 μm slit. The Hg spectra shown in Figure 3(a) are also used to measure the spectral dispersion; the dispersion increases by 25% from 310 nm to the measurement region (0.0043 nm/pxl at 266 nm) due to the change in the grating angle.

To determine the magnification, resolution, and focus of the collection system, a grid with lines parallel to the axis of the probe beam was centered at TCC. The spectrometer is mounted to allow the spectral slit to be rotated parallel to the grid lines at TCC for future imaging Thomson-scattering experiments; Figure 3(b) shows an image of the grid back illuminated by 263 nm laser light when the spectral slits have been rotated to be parallel to the probe beam axis. In this image the spectrometer is rotated by 60 degrees from its nominal vertical position used for streaked Thomson-scattering measurements. Features less than 60μm are visible indicating good spatial resolution. The magnification of the system (M=1.8) is measured by comparing the 1 mm spectral slit width to the 63.5 μm grid spacing in the detector plane. Figure 3(b) shows the system has a large field of view along the probe beam axis (3 mm) that will allow future temperature measurements along the complete 2 mm hohlraum axis (limited by the length of the diagnostic window in the hohlraum wall) on a single shot.

The Thomson-scattering volume (60 μm$\times$110 μm$\times$80 μm) is defined by the beam waist of the probe beam (60 μm) and the projection of the spectrally and temporally resolving slits into the plasma. The Thomson-scattering volume was aligned to the center of the hohlraum using the end of a 100 μm optical fiber located at TCC.

III. RESULTS

The experiments discussed in this section demonstrate the ability of this new target platform to reach ignition relevant electron temperatures approaching 4 keV where laser backscatter, beam deflection, beam filamentation, and self focusing can be studied. Furthermore, these results are used to validate the nonlocal model and benchmark the flux limiter used in the hydrodynamic simulations performed by HYDRA. A flux limiter of $f = 0.05$ matches the experimentally measured electron temperatures made at the center of the CH gas filled hohlraums as a function of time. In this location, the differences between the flux

limited model and the nonlocal model are small. For the electron temperature measurements performed in 1 mg/cc SiO_2 foam, both models used by HYDRA significantly over estimate the electron temperature early in time. Thomson-scattering experiments that measure the electron temperature profile perpendicular to and along the hohlraum axis using significantly less probe energy (while reducing the pulse to keep the same laser power) will reduce the perturbation due to the probe laser and help distinguish between the flux limited diffusion model, nonlocal model [13], and models that include magnetic field effects [12, 15] .

A. CH Gas Filled Hohlraums

Figure 4 shows streaked Thomson-scattering data from the center of a CH-filled hohlraum heated with a total heater beam energy of 13.5 kJ. For the duration of the probe (300 ps to 1300 ps), two symmetric ion-acoustic features are observed from the light scattered off the CH-plasma indicating a nearly Maxwellian distributions. In our CH-plasmas, the solution to the kinetic dispersion relation gives slow and fast ion-acoustic modes which are evident in the Thomson-scattering spectra as fast hydrogen-like and slow carbon-like modes [16, 17].

The wavelength separation between the modes provides a measure of the electron temperature while the total scattered power is a measure of the electron density. The relative damping of the slow and fast modes provides an accurate measure of the ion temperature [16, 20]. The scattering spectrum shown in Figure 4 demonstrates the change in relative damping of the two modes; early in time the hydrogen-like mode is dominant. In the series of spectra that are shown in Figure 4(b-f) the carbon-like mode grows in time indicating an increase in the ratio between the ion and electron temperature. Fitting the data with the Thomson-scattering form factor [19] for a two-ion-species plasma accurately measures the electron density, electron temperature, and ion temperature in the CH plasmas.

Figure 5 shows the temporal evolution of the electron and ion temperatures for a series of heater beam energies. This analysis assumes that the light scattering occurs on a fully ionized CH-plasma which is assured by the high temperatures and confirmed by the hydrodynamic simulations that show a fully ionized CH plasma 100 ps after the start of the heater beams. Temporally resolved two-dimensional x-ray images observing the Au-plasma emission at energies of $E > 2.5$ keV show that the Au-ions are held back by the fill plasma and therefore, do not enter the scattering volume [15]. We find that the electron and ion

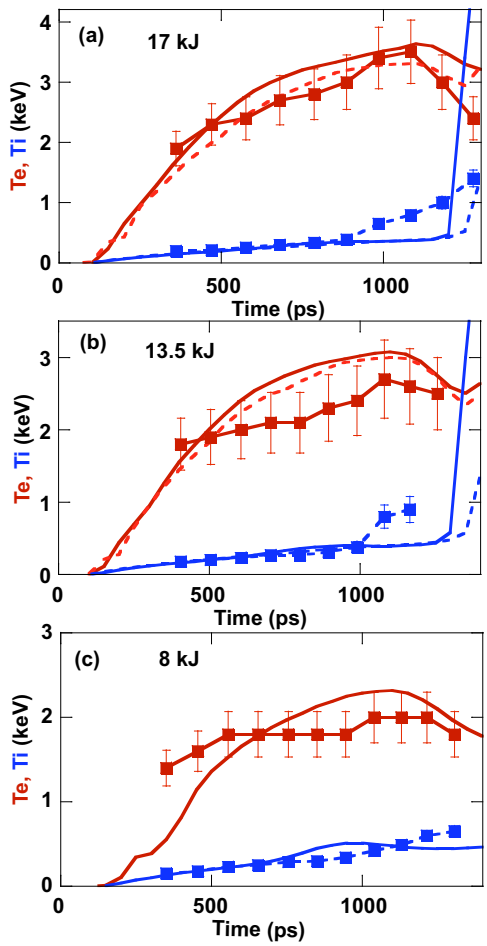

FIG. 5: The electron (red squares) and ion (blue circles) temperatures are measured in a CH-plasma using Thomson scattering at the center of the hohlraum for different total heater beam energies: (a) 17 kJ, (b) 13kJ, (c) 8 kJ. The data are compared to hydrodynamic simulations using either a free streaming flux limited model (solid lines) or a nonlocal model (dashed lines).

temperatures measured with Thomson scattering agree with HYDRA simulations, but single point temperature measurements are not able to distinguish between the two models at this spatial location. Imaging Thomson scattering measurements are required to explore the discrepancy between the models.

The simulated ion temperatures are remarkably similar to the measured results and show an ion temperature much lower than the temperature of the electrons. The temporal evolution of the ion temperature for the different heater beam energies is very similar prior to stagnation (t< 1 ns); this can be explained by the fact that in our simulations the electron-ion equilibration time is much longer than 1 ns. The electron temperature is generally

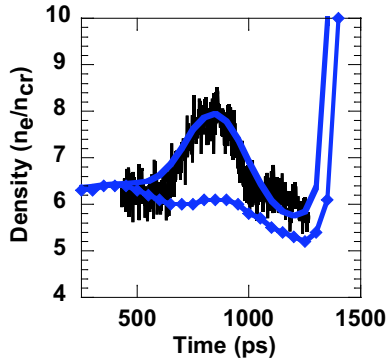

FIG. 6: The relative electron density profile measured (black line) using the power collected in the Thomson-scattering diagnostic is compared with nonlocal (dashed line) and a flux limited (solid line) simulations for a CH-gas filled hohlraum with a total heater beam energy of 13.5 kJ.

determined by the balance between inverse bremsstrahlung heating and conduction losses while the ion temperature is determined by the electron-ion equilibration time and hydrodynamics, therefore, over the time of our experiments, the ion temperature is determined by the electron-ion equilibration rate which is similar for each heater beam energy.

Figure 6 compares the electron density measured using Thomson scattering with the two hydrodynamic models. The power scattered by Thomson scattering is a function of the density allowing the relative density profile to be extracted from the measured intensity profile. By scaling the scattered power measurement at 400ps to $n_e = 5.7 \times 10^{20}$ cm^{-3} the measured profile is compared to the simulations.

The data reflect the large change in the temporal density profile calculated using the flux limited heat transport model with a flux limiter of $f = 0.05$. The initial density peak observed in the flux limited simulation (t$\sim$ 800 ps) is caused by laser-driven blast waves colliding on the hohlraum axis. These waves are thermally driven blast waves launched as the heater beams initially burn through the gas. This density bump is much weaker in the simulation using the nonlocal model. In these simulations, the blast waves are counter acted by the expansion due to the local heating from the probe beam propagating down the hohlraum axis. Late in time ($t > 1300$ ps), the simulations show a stagnation wave entering the Thomson-scattering volume that is driven by the rapid heat expansion of the gold wall. This stagnation is not observed by the experiment as the probe beam is turned off at 1300 ps.

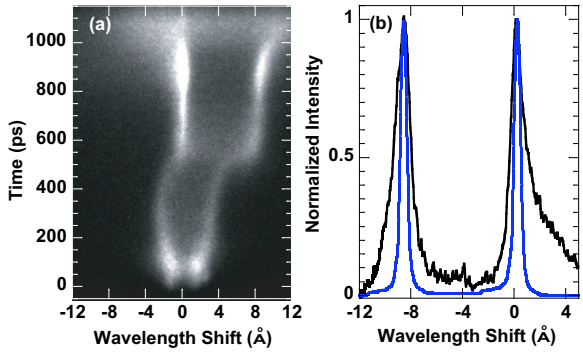

FIG. 7: (a) The steaked Thomson-scattering spectrum for SiO_2 shows narrow ion-acoustic features that are not resolved by the instrument. (b) The form factor fit (blue line) to the spectra yields an electron temperature of $T_e = 4$ keV at t=1.0 ns.

The present experimental study measures the conditions in the center of the target where the nonlocal modeling provides a similar electron temperature as the flux-limited case. Future work is planned to compare these advanced heat transport models with spatially resolved Thomson-scattering measurements. The CH-gas filled target platform has been well characterized and has proven to reach electron temperatures of 3.5 keV.

B. SiO_2 Foam Filled Hohlraums

Current designs for ignition targets at the National Ignition Facility (NIF) also explore the use of foam fills to control the high-Z wall blow-off. The experiments presented in this section use hohlraums that are filled with a 1 mg/cc SiO_2 foam which are shown to produce a peak electron temperature above 4 keV.

Figure 7 shows a Thomson-scattering spectrum where the hohlraum was heated with a total energy of 17 kJ. Ion-acoustic waves are weakly damped in the SiO_2 plasma and, early in time, the scattered spectra show narrow features that are not resolved by the instrument. The separation between the up and down shifted ion-acoustic features provide a direct measure of the electron temperature assuming the SiO_2 plasma is fully ionized.

The spectra is fit using the Thomson-scattering form factor including the measured instrument function (Figure 7(b)). For these parameters, the fit is not sensitive to the ion temperature. Late in time the spectra broadens indicating an increase in gradients within the Thomson-scattering volume ($\Delta v/v$=10%). This increase in gradients is a signature of

the beginning of stagnation; the shock wave is launched by the rapid expansion of the gold wall.

Figure 8 compares the measured electron temperature evolution with the hydrodynamic simulations for two heater beam conditions. The simulated electron temperature profile in SiO_2 does not match the data as well as the CH-gas filled simulations. This is likely due to the fact that HYDRA simulates the foam as a gas, and therefore does not include the correct physics of laser absorption which starts as a bunch of tiny solid SiO_2 filaments.

The symmetry around the frequency of the probe laser shown in Figure 7(a) for early times indicates very little particle flow; at 500 ps the flow is rapidly increased to Mach 1 correlated with the rapid increase in electron temperature. The Mach 1 flow observed in the SiO_2 foam filled targets may be a signature of non-uniformity in the foam density or a result of the hydrodynamics involved with the exploding filaments. The simulated flow in the direction of the probed ion-acoustic wave is very small. The differences in the early time electron temperatures between the two material fills are likely a result of the fact that the SiO_2 electron density is half the electron density in the CH gas.

C. Heater Beam Scaling

Figure 9 demonstrates the ability to control the peak electron temperature by varying the heater beam energy deposited into the hohlraum. In our targets, the electron temperature along the hohlraum axis is determined by the elctron temperature at the gold-gas interface where the the pressure in the gas ($n_e T_e$) is balanced with the x-ray ablation pressure created by the radiation wave propagating into the cold gold wall. As the conductivity is fairly high in the gas, the temperature in the gas is fairly uniform and determined by the temperature at this interface.

The small difference between the simulated electron temperature using the nonlocal and flux limited simulations make it difficult for the data to distinguish between the models. In the SiO_2 foams the simulations show the nonlocal model predicting higher electron temperatures than the flux limited model while the effect is reversed in the CH simulations. Furthermore, the simulations seem to better predict the electron temperature in the gas filled hohlraums.

The ability to scale the electron temperature in these long-scale length plasmas will

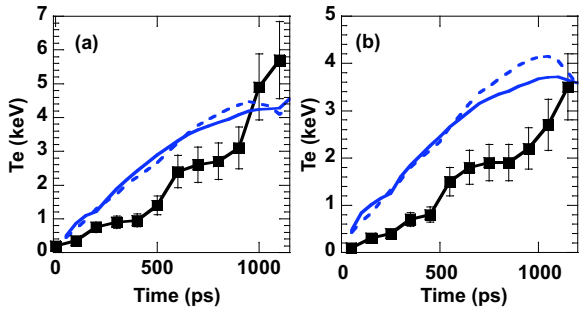

FIG. 8: (a) The measured electron temperature time history (squares) for a total heater energy of (a) 17 kJ and (b) 13 kJ is compared to the hydrodynamic simulations using a flux limited model (solid line) and a nonlocal model (dashed line). The hohlraums were filled with 1 mg/cc SiO_2.

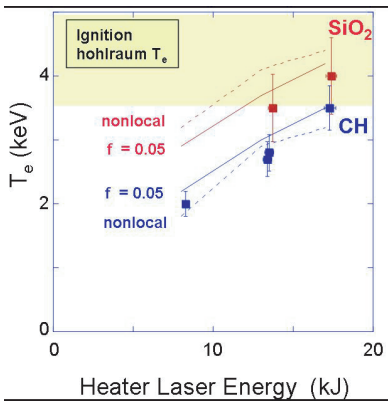

FIG. 9: Changing the heater beam energy allows the peak electron temperature to be selected in a hohlraum filled with S_iO_2 foam (red) or CH gas (blue). Hydrodynamic simulations are performed using a flux limiter of $f = 0.05$ (solid line) and a nonlocal model (dashed line). The data are averaged over 200 ps.

allow laser-plasma interaction studies to be performed where $k\lambda_{De}$ can be compared to previous results using gas bag targets and then scaled to a new high-temperature regime ($k_{epw}\lambda_{De} > 0.54$) where theories predict a loss of resonance for stimulated Raman scattering resulting in a significant drop in reflectivity [? ?].

IV. CONCLUSIONS

We have demonstrated high electron temperatures with Thomson scattering in a new target platform that will be used to study laser plasma interactions. Scaling the total heater

beam energy between 8 kJ and 17 kJ has demonstrated the ability to vary the plasma conditions along the axis of the hohlraum. This allows laser-plasma interaction experiments to be performed along the hohlraum axis in a long 2 mm scale length plasma with the capacity to reach temperatures between 3 keV and 4 keV comparable to those expected for indirect drive ICF.

Future interaction studies with probe beams at both 2ω and 3ω will use this new target platfrom to determine the limitations on electron temperature, density, and intensity for efficient beam propagation [21]. Further studies with this target platform are directed to differentiate between hydrodynamic models and the importance of magnetic fields through measurements of the spatial temperature gradients parallel and perpendicular to the hohlraum axis using imaging Thomson scattering techniques [22].

We would like to acknowledge the efforts of W. Armstrong and the Omega Laser Crew. We thank D. Hargrove and his technical team for their contributions to fielding the Thomson-scattering diagnostic and R. Kirkwood for discussions regarding the optical configuration. Furthermore, we thank R. Griffith and the NIF for the streak camera support. This work was supported by LDRD 06-ERD-056 and was performed under the auspices of the U.S. Department of Energy by the Lawrence Livermore National Laboratory under Contract No. W-7405-ENG-48.

---

[1] J. D. Lindl, P. A. Amendt, R. L. Berger, S. G. Glendinning, S. H. Glenzer, S. W. Haan, R. L. Kauffman, O. L. Landen, and L. J. Suter, Phys. Plasmas **11**, 339 (2004).

[2] S. H. Glenzer, K. B. Fournier, C. B. Decker, B. A. Hammel, R. W. Lee, L. Lours, B. J. MacGowan, and A. L. Osterheld, Physical Review E **62** (2000).

[3] J. C. Fernandez, B. S. Bauer, K. S. Bradley, J. A. Cobble, D. S. Montgomery, R. G. Watt, B. Bezzerides, K. G. Estabrook, R. Focia, S. R. Goldman, et al., Phys. Rev. Lett. **81**, 2252 (1998).

[4] K. B. Fournier, C. Constantin, C. A. Back, L. J. Suter, H. K. Chung, M. C. Miller, D. H. Froula, G. Gregori, S. H. Glenzer, and O. L. Landen (2005).

[5] J. D. Lindl, Phys. Plasmas **2**, 3968 (1995).

[6] et. al. Sources, Fusion Technol. **30**, 492 (1996).

[7] A. J. MacKinnon, S. Shiromizu, G. Antonini, J. Auerbach, H. Haney, D. H. Froula, J. Moody, G. Gregori, C. Constantin, C. Sorce, et al., Rev. Sci. Instrum. **75**, 3906 (2004).

[8] N. B. Meezan, L. Divol, M. M. Marinak, G. D. Kerbel, L. J. Suter, R. M. Stevenson, E. Slark, and K. Oades, Phys. Plasmas **11**, 5573 (2004).

[9] M. M. Marinak, G. D. Kerbel, N. A. Gentile, O. S. Jones, D. H. Munro, S. Pollaine, T. R. Dittrich, and S. W. Haan, Phys. Plasmas **8**, 2275 (2001).

[10] L. Spitzer and R. Harm, Physical Review **89**, 977 (1953).

[11] Y. T. Lee and R. M. More, Phys. Fluids **27**, 1273 (1984).

[12] P. Nicolai, M. Vandenboomgaerde, B. Canaud, and F. Chaigneau, Phys. Plasmas **7**, 4250 (2000).

[13] J. F. Luciani, P. Mora, and J. Virmont, Phys. Rev. Lett. **51**, 1664 (1983).

[14] G. P. Schurtz, P. Nicolai, and M. Busquet, Phys. Plasmas **7**, 4238 (2000).

[15] S. H. Glenzer, W. E. Alley, K. G. Estabrook, J. S. D. Groot, M. G. Haines, J. H. Hammer, J. P. Jadaud, B. J. MacGowan, J. D. Moody, W. Rozmus, et al., Phys. Plasmas **6** (1999).

[16] S. H. Glenzer, C. A. Back, K. G. Estabrook, R. Wallace, K. Baker, B. J. MacGowan, B. A. Hammel, R. E. Cid, and J. S. D. Groot, Phys. Rev. Lett. **77**, 1496 (1996).

[17] D. H. Froula, L. Divol, H. A. Baldis, R. L. Berger, D. G. Braun, B. I. Cohen, R. P. Johnson, D. S. Montgomery, E. A. Williams, and S. H. Glenzer, Phys. Plasmas **9**, 4709 (2002).

[18] D. H. Froula, L. Divol, D. G. Braun, B. I. Cohen, G. Gregori, A. Mackinnon, E. A. Williams, S. H. Glenzer, H. A. Baldis, D. S. Montgomery, et al., Phys. Plasmas **10**, 1846 (2003).

[19] D. E. Evans, Plasma Physics **12**, 573 (1970).

[20] D. H. Froula, L. M. Divol, and S. H. Glenzer, Phys. Rev. Lett. **88**, 105003 (2002).

[21] C. Niemann, S. H. Glenzer, J. Knight, L. Divol, E. A. Williams, G. Gregori, B. I. Cohen, C. Constantin, D. H. Froula, D. S. Montgomery, et al., Phys. Rev. Lett. **93**, 045004 (2004).

[22] G. Gregori, S. H. Glenzer, J. Knight, C. Niemann, D. Price, D. H. Froula, M. J. Edwards, R. P. J. Town, W. Rozmus, A. Brantov, et al., Phys. Rev. Lett. **92** (2004).

This work was performed under the auspices of the U. S. Department of Energy by University of California, Lawrence Livermore National Laboratory under contract W-7405-Eng-48.